

1 **Tailored on demand anti-coagulant dosing: an *in vitro* and *in***  
2 ***vivo* evaluation of 3D printed purpose-designed oral dosage**  
3 **forms**

4  
5 Basel Arafat<sup>1,2</sup>, Nidal Qinna<sup>3</sup> Milena Cieszynska<sup>1</sup>, Robert T Forbes<sup>1</sup>, Mohamed A  
6 Alhnan<sup>1\*</sup>

7  
8 <sup>1</sup> School of Pharmacy and Biomedical Sciences and <sup>2</sup> School of Medicine, University of Central  
9 Lancashire, Preston, Lancashire, UK.

10 <sup>2</sup> Faculty of Medical Sciences and Public health, Anglia Ruskin University, Chelmsford, UK

11 <sup>3</sup> Faculty of Pharmacy and Medical Sciences, University of Petra, Amman, Jordan.

12  
13  
14  
15  
16  
17 \*Corresponding author: [MAIbedAlhnan@uclan.ac.uk](mailto:MAIbedAlhnan@uclan.ac.uk)

## 26 ABSTRACT

---

27 Coumarin therapy has been associated with high levels of inter- and intra-individual  
28 variation in the required dose to reach a therapeutic anticoagulation outcome.  
29 Therefore, a dynamic system that is able to achieve accurate delivery of a warfarin  
30 dose is of significant importance. Here we assess, the ability of 3D printing to fabricate  
31 and deliver tailored individualised precision dosing using an in-vitro model. Sodium  
32 warfarin loaded filaments were compounded using hot melt extrusion (HME) and  
33 further fabricated *via* fused deposition modelling (FDM) 3D printing to produce  
34 capsular-ovoid-shaped dosage forms loaded at 200 and 400 µg dose. The solid  
35 dosage forms and comparator warfarin aqueous solutions were administered by oral  
36 gavage to Sprague–Dawley rats. *In vitro*, warfarin release was faster at pH 1.2 in  
37 comparison to pH 2. A novel UV imaging approach indicated that the erosion of the  
38 methacrylate matrix was at a rate of 16.4 and 15.2 µm/min for horizontal and vertical  
39 planes respectively. *In vivo*, 3D printed forms were as proportionately effective as  
their comparative solution form in doubling plasma exposure following a doubling of  
warfarin dose (184% versus 192% respectively). The 3D printed ovoids showed a  
lower C<sub>max</sub> of warfarin (1.51 and 3.33 mg/mL versus 2.5 and 6.44 mg/mL) and a longer  
T<sub>max</sub> (6 and 3.7 versus 4 and 1.5 h) in comparison to liquid formulation. This work  
demonstrates for the first time *in vivo*, the potential of FDM 3D printing to produce a  
tailored specific dosage form and to accurately titrate coumarin dose response to an  
individual patient.

---

40 **Keywords:** *Rapid prototyping; Patient-centred; Personalized; Patient-specific; Three*  
41 *dimensional printing; additive manufacturing.*

42

43

## 44 1. Introduction

45 For over 50 years now, coumarins have been the most prescribed oral anticoagulants.[1]  
46 Nevertheless, despite their wide use, coumarin therapy has been associated with a high level of  
47 inter-individual variation in dose required to achieve therapeutic anticoagulation response.[2]  
48 The administration of an inappropriate warfarin dose for example may place a patient in a  
49 hypercoagulable state or increase the patient's risk of bleeding complications early in therapy.  
50 As a consequence of over-anticoagulation response, there is an increased risk of major bleeding  
51 following the use of anticoagulants by 9.1% [3]. The American College of Chest Physicians  
52 (ACCP) supports an “induction” dose of 2 to 5 mg per day which needs to be adjusted  
53 according to the patient's International Normalised Ratio (INR)[4]. The pharmacodynamics  
54 and pharmacokinetics of coumarins are largely influenced by many factors such as patient age,  
55 body weight, dietary vitamin K intake, concomitant medications, as well as various disease  
56 states.[2] Hence to ensure that the patient's INR remains within the target range, regular  
57 coagulation monitoring and dose modification is necessary.[5]

58 Nevertheless, limited doses of warfarin tablets are available in the market and dose  
59 modification usually requires multiple tablet ingestion or cutting or splitting of larger dose  
60 tablets, which could lead to variations in drug content.[6, 7] An area of potential improvement  
61 to warfarin therapy would be the ability to produce flexible on-demand precision tailored dose  
62 adjustments (particularly given warfarin's due to narrow therapeutic index). One technology  
63 that can potentially easily benefit anticoagulant therapy is 3D printing, owing to its flexible and  
64 precise manufacturing capability, which enables administration of the lowest effective dose of  
65 the drug to maintain the target INR. Indeed, recently, Vuddanda et al. (2017) demonstrated the  
66 potential of a re-engineered thermal inkjet printer to address the challenge of warfarin dosage  
67 personalisation, achieving highly reproducible minute warfarin dose of approximately 50 µg  
68 [8]

69 3D printing potential and feasibility has been revealed in several fields such as aerospace,  
70 engineering, arts, as well as in fabricating medical implants and devices. Although still at its  
71 infancy in the field of personalised medicine, it is expected to revolutionise healthcare and set  
72 an innovative platform for pharmaceutical product design and extemporaneous preparation of  
73 patient-tailored dosage forms.[9] Fused deposition modelling (FDM) 3D printing, in particular,  
74 has been proposed as a platform for controlling the dose.[10] It has demonstrated its capability  
75 to manufacture mechanically stable tablets fabricated from pharmaceutical grade polymers  
76 without post-processing steps.[10-13] For instance, FDM 3D printing has been viably  
77 established using pharmaceutical grade polymers such as PVP [9, 14], methacrylate [15] and  
78 cellulose [12] based polymers.

79 The use of animal models is commonly used to predict formulation behaviour in humans.  
80 The use of rats in particular is favoured due to their small size, relatively low cost of breeding  
81 and up-keep, as well as the presence of large databases of drug pharmacokinetic data in rats  
82 and in humans.[16] Nevertheless, the testing of solid dosage forms in rats presents a challenge  
83 in terms of ease of administration. Owing to the need to use a small dosage form size, crushed  
84 tablets filled in capsule or suspended in liquid have often been used as an inferior alternative  
85 to test the *in vivo* performance of a tablet in rats.[17, 18] However, such approaches  
86 significantly alter the nature of the dosage form. More recently, the formulation of mini-tablets  
87 for animal use have been attempted [19, 20]. It is therefore important to develop strategies that  
88 authentically test intact scaled down human dosage forms for animal studies to enable more  
89 reliable extrapolation of human pharmacokinetic responses.

90 This work aimed to assess the suitability of FDM 3D printer technology for i) fabricating  
91 purposely designed solid dosage forms, and ii) tailoring the dose of a narrow therapeutic index  
92 drug, namely warfarin. To achieve this goal, rat-tailored FDM 3D printed warfarin ovoid  
93 tablets were printed and administered to Sprague–Dawley rats for testing to obtain their  
94 pharmacokinetics (PK) parameters.

## 95 2. Materials and methods

96

### 97 2.1 Materials

98 Warfarin (sodium salt) was purchased from Arcos (UK). Eudragit E was donated from  
99 Evonik Industries (Darmstadt, Germany). Triethyl citrate (TEC) and tri-calcium phosphate  
100 (TCP) were supplied by Sigma–Aldrich (UK). Acetonitrile and methanol were supplied by  
101 British Drug Houses (BDH, London, UK). Scotch Blue Painter’s tape 50 mm was supplied by  
102 3M (Bracknell, UK).

### 103 2.2 Preparation and optimisation of filaments

104 In order to fabricate drug-loaded filaments, a hot melt extrusion method was implemented  
105 using a Thermo-Scientific HAAKE MiniCTW extruder (Karlsruhe, Germany). A 10 g sample  
106 of Eudragit E: TEC: TCP: sodium warfarin 46.75 : 3.25 : 49:1) was accurately weighed and  
107 added gradually to counter flow twin-screw hot melt extruder, HAAKE MiniCTW (Karlsruhe,  
108 Germany). To allow homogeneous distribution of the powders, the molten mass was mixed in  
109 the extruder for at least 5 min prior to extrusion. The specific temperature of initial feeding and  
110 extrusion for the filament were 100 and 90 °C respectively. A torque control of 0.8 Nm was  
111 used to extrude the filaments. Filaments were stored in sealed plastic bags at room temperature  
112 before 3D printing.

### 113 2.3 Design and printing of tablets

114 Tablets were constructed with the pre-prepared filaments using a MakerBot Replicator<sup>®</sup> 2X  
115 Experimental 3D Printer (MakerBot Industries, New York, USA) equipped with 0.4 mm  
116 nozzle size. The templates used to print the tablets were designed in a caplet shape using  
117 Autodesk<sup>®</sup> 3ds Max<sup>®</sup> Design 2016 software version 18.0 (Autodesk, Inc., USA). The design  
118 was saved in a stereolithography (.stl) file format and was imported to the 3D printer’s  
119 software, MakerWare Version 3.9.1.1143 (Makerbot Industries, LLC., USA).

120 Two sets of 3D printed tablets were fabricated:

121 In order to establish the ability of the system to control the low dose of drug for clinical  
122 use, a series of tablets with increasing volumes were then printed by increasing the dimensions  
123 of the design: length × width × heights (L, H, W). The ratios between dimensions  
124 ( $W = H = 0.4 L$ ) remained constant. The size of the printed tablet ( $M$ ) was changed to achieve  
125 target doses of 0.5, 1, 3 or 5 mg (Table 1S).

126 To assess *in vivo* performance of this tablets in rats, a separate set of 3D printed ovoid  
127 shapes were manufactured with a cylindrical diameter of 2 mm and lengths of 5.5 or 11 mm to  
128 achieve a dose of 200 and 400µg respectively. Objects were printed using modified settings of  
129 the software as described earlier in our previous work at a temperature of 135 °C. [15]

### 130 2.4 Thermal analysis

131 Samples (raw materials, extruded filaments and printed tablets) were characterised using  
132 differential scanning calorimetry (DSC) and thermogravimetric analysis (TGA). For DSC  
133 analysis, a differential scanning calorimeter DSC Q2000 (TA Instruments, Elstree,  
134 Hertfordshire, UK) with a heating rate of 10 °C/min was used. Samples were heated to 100 °C  
135 for 5 min to exclude the effect of humidity then cooled to -20 °C. This was followed by a heat  
136 scan from -20 °C to 300 °C. Analysis was carried out under a purge of nitrogen (50 mL/min).  
137 The data was analysed using TA 2000 analysis software. Standard 40 µL TA aluminium pans  
138 and pin-holed lids were used with an approximate sample mass of 5 mg. All measurements  
139 were carried out in triplicate.

140 For TGA analysis, raw materials, extruded filaments and 3D printed tablets were analysed  
141 using a TGA/SDTA851e Mettler Toledo (Leicester, UK). Samples (5 mg, n=3) were placed in  
142 40 µL aluminium pans and were then heated from 25 to 500 °C at a heating rate of 10°C/min  
143 and nitrogen gas flow of 50 mL/min. The thermal decomposition (or degradation) profile was  
144 analysed using STARE software version 9.00.

## 145 146 2.5 X-ray powder diffraction (XRD)

147 Samples (raw materials extruded filaments and printed tablets) were characterised using  
148 an X-ray diffractometer, D2 Phaser with Lynxeye (Bruker, Germany). Samples were scanned  
149 from  $(2\theta)= 5^\circ$  to  $50^\circ$  using  $0.01^\circ$  step width and a 1 second time count. The divergence slit was  
150 1 mm and the scatter slit 0.6 mm. The wavelength of the X-ray was 0.154 nm using Cu source  
151 and a voltage of 30 kV. Filament emission was 10 mA using a scan type coupled with a  
152 theta/theta scintillation counter over 60 min.

## 153 154 2.6 Characterisation of tablet properties

155 The hardness of six ovoid tablets was measured using a TBH 200 (Erweka GmbH,  
156 Heusenstamm, Germany). The mean crushing strength was determined, whereby an increasing  
157 force was applied to the tablet until it fractured or deformed.

158 In order to assess the friability of the tablets, 20 tablets were randomly selected, weighed  
159 and placed in a friability tester Erweka TAR 10 (Erweka GmbH, Heusenstamm, Germany) and  
160 the drum was then rotated at 25 rpm for 4 min. The tablets were reweighed and the differences  
161 in weight were calculated and displayed as a percentage of the original sample weight. In order  
162 to assess weight uniformity, 10 tablets were randomly selected and weighed. The average  
163 weights were measured and the percentage deviation of the individual tablets from the mean  
164 was determined.

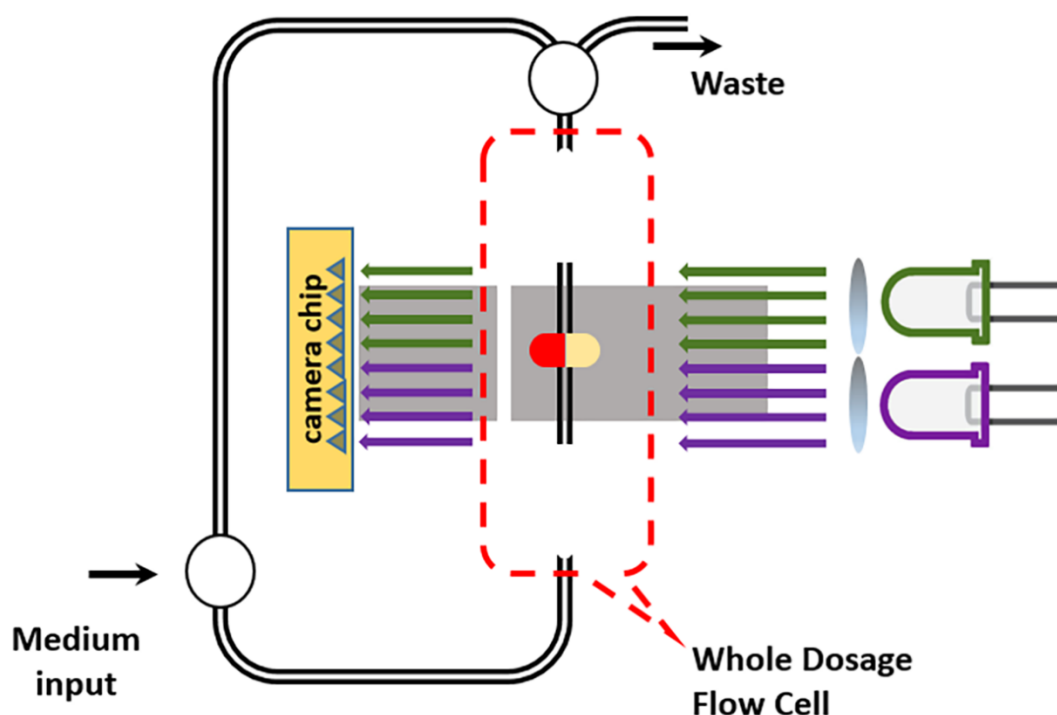
165 To assess the impact of both HME and FDM 3D printing on drug content, 3 tablets from  
166 each formulation, were randomly selected and weighed. Tablets were then individually placed  
167 in a 1000 mL volumetric flask containing 0.1 M HCl and sonicated for 2 h. The solutions were  
168 filtered through 0.22 µm Millex-GP syringe filters (Merck Millipore, USA) and prepared for  
169 HPLC analysis.

170 Warfarin concentration in samples was assessed using an Agilent UV-HPLC 1260 series  
171 (Agilent Technologies, Inc., Germany) equipped with Kinetex C18 column ( $100 \times 2.1$  mm,  
172 particle size 2.6 µm) (Phenomenex, Torrance, USA) and set at temperature 26 °C. The mobile  
173 phase was 4:1 mixture of methanol: pH 3 water (adjusted with orthophosphoric acid) at a flow  
174 rate of 1 mL/min. The injection volume was 100 µL and the stop time was 10 min. The

175 wavelength was set to 230 nm and the retention time of the drug was 6.3 min with a limit of detection  
176 of 0.05 mg/L.

## 177 2.7 *In vitro* dissolution studies.

178 a. Surface dissolution imaging. A Sirius SDi2, the second generation UV imaging system,  
179 designed to accommodate whole dosage forms, was used to visualize surface dissolution of  
180 sodium warfarin from the 3D printed dosage forms as a whole (Fig. 1). The 3D printed tablets  
181 were introduced into the SDi2's flow cell. The dissolution medium (0.1M HCl at 37°C) applied  
182 at a flow rate of 8.2 mL/min. The dissolution medium was introduced into the flow cell in the  
183 open loop configuration, from bottom to top, with an equivalent linear velocity of 1 cm/min.  
184 Dissolution experiments were recorded for a total duration of 60 min. The two dimensional  
185 detection area on the SDi2 is significantly larger than for the SDI (24 mm width x 28 mm  
186 height) to accommodate dissolution imaging profiling of intact whole dosage forms, with a  
187 spatial resolution of 13.75  $\mu\text{m}$ . The flow cell was illuminated using alternate pulses from two  
188 255 and 520 nm wavelength LEDs. The dual wavelength enables two separate video captures  
189 to be produced from a single experiment. Real-time data were then used to measure and  
190 differentiate between drug release into solution and tablet erosion from the 255 and 520 nm  
191 light obtained videos, respectively.



192

193 **Figure 1.** Schematic diagram of SDi2 instrument. LED's of different wavelength are employed to  
194 illuminate the 3D printed tablet in flow through cell filled with gastric medium. The obscuration or  
195 absorbance of the sample was recorded using an Actipix detector. The medium is pre-heated to 37°C  
196 before going through the Whole Dosage Flow Cell and is recirculated in a closed loop configuration.

197 b. USP II dissolution studies. The *in vitro* release of warfarin from 3D printed tablets was  
198 investigated using a USP II Erweka DT600 dissolution tester (Erweka GmbH, Heusenstamm,

199 Germany). Three tablets were randomly selected and individually placed in the dissolution  
200 vessels each containing 900 mL of a fasted state simulated gastric fluid (FaSSGF) (1.75 mM  
201 SLS, 0.01N HCl, 0.2% NaCl, pH 2.0) at 50 rpm and  $37 \pm 0.5$  °C. Aliquots (5 mL) were  
202 manually collected using 5 mL Leur-Lock syringes at 0, 5, 10, 15, 20, 25, 30, 40, 50 and 60 min  
203 time intervals and filtered through an Agilent 0.22  $\mu$ m filter. Each aliquot withdrawn was  
204 replaced with 5 mL of 0.1 M HCl and analysed using the above described HPLC method.

## 205 2.8 *In vivo* studies

206 Adult healthy male Sprague–Dawley rats with an average weight of  $240 \pm 15$  g  
207 accommodated at the University of Petra's Animal House (Amman, Jordan) under controlled  
208 temperature (22 °C–24 °C), humidity (55%–65%), and a 12 hours photoperiod cycle. All rats  
209 were acclimatized for 10 days before experimentation. Rats were weighed and randomized into  
210 groups (n=6 rats per cage). Rats were offered standard pellet diet (Jordan Feed Company Ltd.,  
211 Amman, Jordan) and served clean tap water ad libitum. However, animals were fasted for 18  
212 hours before the day of testing. All experiments were carried out in accordance with University  
213 of Petra's Institutional Guidelines on Animal Use that adopts the guidelines of the Federation  
214 of European Laboratory Animal Sciences Association (FELASA). The animal study protocols  
215 were revised and approved by the Higher Research Council at the Faculty of Pharmacy and  
216 Medical Sciences, University of Petra (Amman, Jordan).

217 3D printed tablets (200 or 400  $\mu$ g) were administered to the rats *via* any oral capsule stainless  
218 steel feeding needle. Comparison control 1 mL warfarin solutions (200 or 400  $\mu$ g), equivalent  
219 to the tablet doses, were freshly prepared and administered to the rats by a stainless steel oral  
220 gavage needle (Harvard Apparatus, Kent, UK). Following oral administrations, blood samples  
221 were pooled from rat's tail (n=6 rats per group) at different time intervals namely at; 1, 2, 3, 4,  
222 6 and 8 hours post administration. Blood was left to clot, centrifuged for 10 min at 2000G, and  
223 then serum was separated and transferred directly into Eppendorf tubes, and kept in a freezer  
224 at  $-20$  °C until analysis.

## 225 2.9 Analysis of warfarin

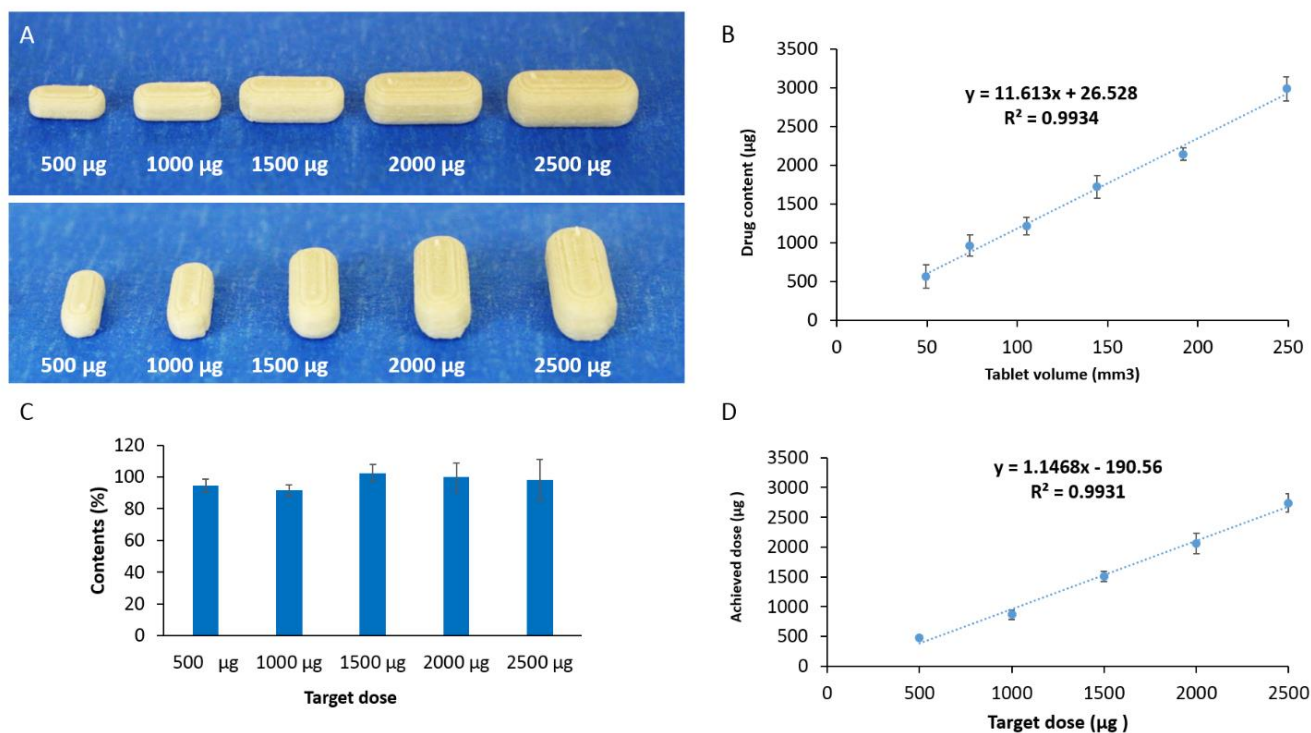
226 For the analysis of warfarin an MS/MS system: API 3200 (Applied Biosystems, MDS  
227 SCIEX, USA) attached to Agilent 1200 HPLC (Agilent Technologies, USA) controlled by  
228 Analyst 1.6.1 software, was utilised. For the extraction of warfarin from the samples, 100  $\mu$ L  
229 of spiked/blank plasma were pipetted into previously labelled Eppendorf tube, 25  $\mu$ L of the  
230 internal standard (IS) Fenofibric acid (FFA) from 100.0  $\mu$ g FFA/mL IS solution was added to  
231 the tubes and vortexed for 30 sec. Afterwards, the precipitation solution, acetonitrile (400.0 $\mu$ L)  
232 was added to the tube and vortexed for further 1 min. Samples were then centrifuged for 5 min  
233 at 14,000 rpm and the supernatant was collated and transferred into an auto-sampler micro vial  
234 for analysis. The mobile phase used for analysis comprised of (30:70) mixture of ammonium  
235 chloride 0.001M: acetonitrile respectively eluted at a flow rate of 0.7 mL/min through a  
236 Thermo BDS Hypersil C18 (50 $\times$ 2.1 mm, particle size 5  $\mu$ m) column (Thermo Fisher Scientific,  
237 Germany) at the temperature 30°C. The injection volume was 5  $\mu$ L and the stop time was  
238 0.7 min. The retention time of the drug was 0.3 min with a limit of detection of 10 ng/mL.

## 239 2.10 Statistical Analysis

240 Independent sample T-test was also employed using a SPSS Software (22.0.0.2) to analyse  
241 the *in vitro* tablet characterisation results. Differences in results where  $p \leq 0.05$  were considered  
242 significant.

243 **3. Results and discussion**

244 In this study, we explored the adaptability of FDM based 3D printing to engineer and control  
 245 the dose of immediate release warfarin tablets. When a series of warfarin tablets with increasing  
 246 dimensions were printed (Fig. 2A, Table S1), a high level of correlation was identified between  
 247 the theoretical volume of the tablet design and their weights ( $R^2=0.9934$ ) (Fig. 2B). This  
 248 indicated the ability of FDM 3D printing method to achieve a sufficient control of the mass of  
 249 3D printed tablets. To establish the ability of such 3D printing method to control dosage,  
 250 theoretical doses based on tablet mass and measured dose of warfarin in the tablet were  
 251 compared. The range of dose accuracy was between 91.5% and 102.4% (Fig. 2C). The  
 252 coefficient of determination between target and achieved dose ( $R^2 = 0.9902$ ) showed that it is  
 253 possible to fabricate tablets with desired dose of warfarin through volume modification even  
 254 at a minute dose of 500  $\mu\text{g}$  (Fig. 2D). With the advances in 3D printers, additional safeguards  
 255 and quality control mechanisms can be introduced to the evolving technology [21], which are  
 256 expected to minimise dose variation in the near future.  
 257

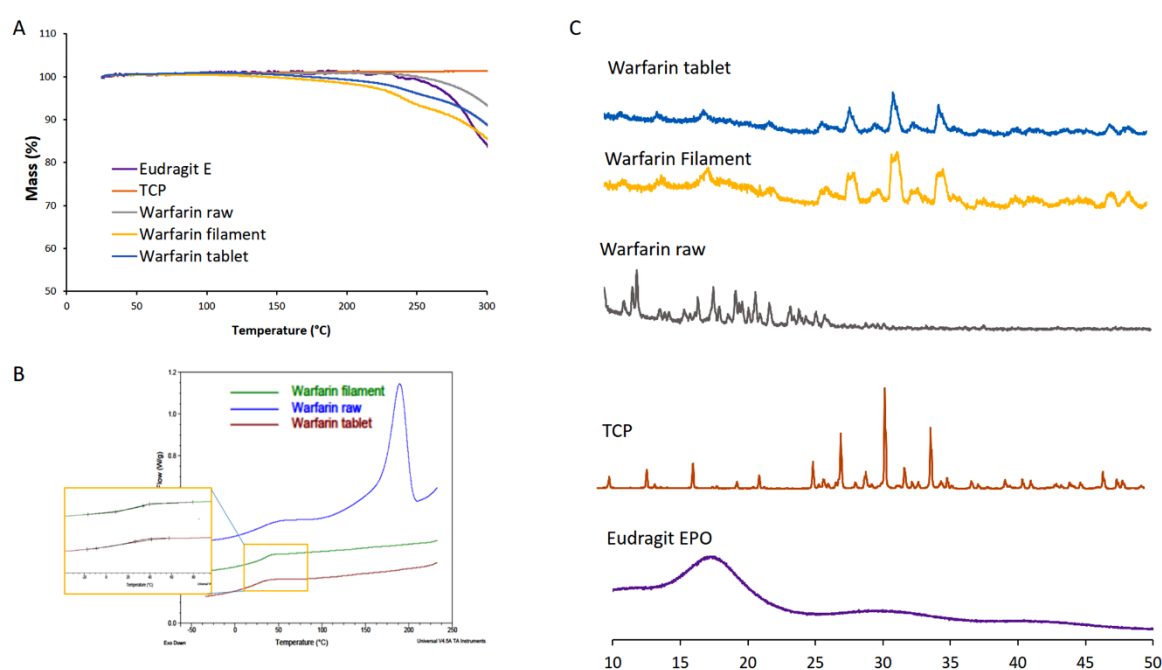


258 **Figure 2.** Precision of 3D printing to control low dose sodium warfarin. (A) Images of warfarin  
 259 loaded FDM 3D printed tablets with increasing dose, (B) Correlation between the theoretical volume  
 260 and tablet mass, (C) warfarin dose accuracy in the 3D printed tablets and (D) correlation between  
 261 theoretical volume and warfarin dose ( $n=3, \pm\text{SD}$ ).

262 Profiles from thermogravimetric analyses of warfarin and other additives as well as HME  
 263 processed filaments and 3D printed tablets are shown in Fig. 3A. Sodium warfarin alone or  
 264 incorporated in filaments did not suffer a significant weight loss at the printing temperature  
 265 135  $^{\circ}\text{C}$ . Therefore, it can be assumed that minimal or no degradation of warfarin occurs in the  
 266 HME as well as in the FDM's nozzle under the utilised temperatures (Fig. 3A). The processing  
 267 temperatures were lower than the melting point of sodium warfarin (161  $^{\circ}\text{C}$ ). Differential  
 268 scanning calorimetry was also conducted to examine the plasticising effect of components on  
 269 the methacrylic filament. As demonstrated in Fig 3B, the addition of TEC as a plasticizer  
 270 significantly depressed the  $T_g$  of filament to 34  $^{\circ}\text{C}$  from 54 $^{\circ}\text{C}$ . However, warfarin was found

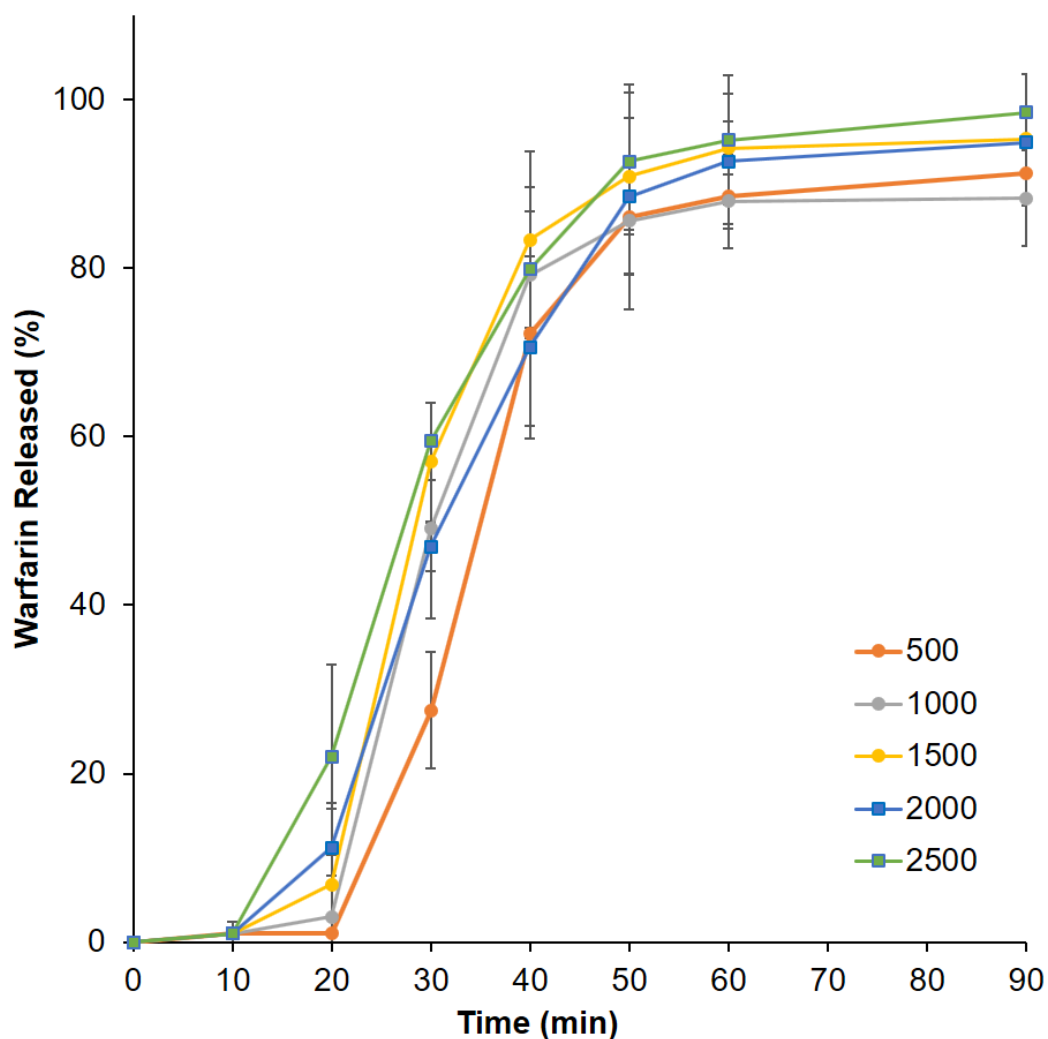
271 to have no significant effect on the Tg of Eudragit E. This could be attributed to the minute  
272 percentage of the drug used in the polymeric structure (1% w/w), which was insufficient to  
273 significantly influence the mobility of methacrylic polymer chains within the filament matrix.  
274 XRD spectra showed that  $\beta$ -calcium tribasic phosphate displayed peaks at 2-theta=17°, 27.8°,  
275 31°, 34.4° corresponding to calcium tribasic phosphate [22], whilst warfarin drug substance  
276 showed peaks at 2-theta=12.4° and 18°. XRD spectra of the warfarin filament and tablet  
277 showed an absence of these specific peaks [23, 24], suggesting the warfarin is present in an  
278 amorphous form within the tablet structure (Fig. 3C).

279 From determination of the mechanical properties of the 3D printed tablets, the friability of  
280 all batches was found to be zero percent. This highlights a prime advantage of FDM 3D printing  
281 in generating mechanically stable tablets over its rival technologies such as extrusion 3D  
282 printing [25] and powder-based 3D printing. [26, 27] The lack of a drying step or any post-  
283 printing finishing procedures, clearly demonstrates the potential of this technology to instantly  
284 produce a ready-to-use dosage form within minutes following a healthcare team request.



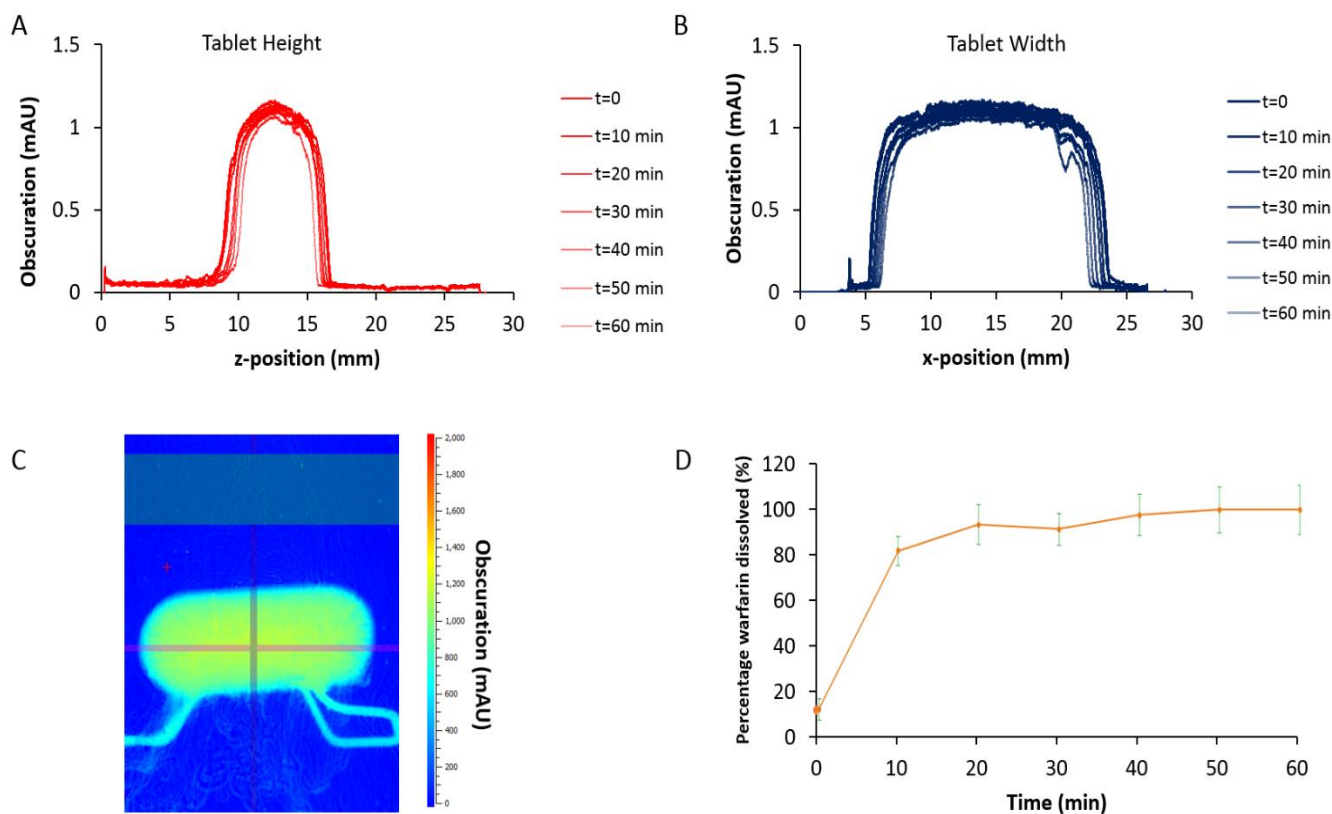
285  
286 **Figure 3.** Thermal analysis of Eudragit E based 3D printing filaments. **(A)** Thermal degradation profiles  
287 for Eudragit E, sodium warfarin, TCP, warfarin loaded filament and tablet, **(B)** DSC thermograph for  
288 warfarin loaded filament and tablet, **(C)** XRD spectra of Eudragit E, TCP, warfarin, and warfarin loaded  
289 filament and tablet.

290  
291 The release pattern of warfarin from the methacrylic matrix was investigated using a  
292 modified FaSSGF [28] as a dissolution medium (Fig. 4). All tablets showed a release pattern  
293 of > 80% dissolution at 45 min regardless of their individual sizes. The dissolution release  
294 profile was attributed to the ionisation of the amino groups of the cationic methacrylic polymer  
295 in modified FaSSGF (pH 2.0), which leads to electrostatic repulsion between cationic polymer  
296 chains and facilitates polymer dissolution and drug release. The release was compliant with  
297 British Pharmacopeia criteria for warfarin tablets [29].



298  
 299 **Figure 4.** *In vitro* release pattern of sodium warfarin from 3D printed tablets of different doses from a  
 300 USPII dissolution test in modified FaSSGF (pH 2.0) (n=3,  $\pm$ SD).

301 To better understand the drug release from the 3D printed tablets, the dissolution behaviour  
 302 of the tablets at the dissolving surface in contact with the dissolution media was explored. A  
 303 single wavelength system has been previously used to study drug powder dissolution [30]. Here  
 304 we employ a UV imaging technology capable of generating visual images from simultaneous  
 305 spectroscopic evaluation for a complete dosage form (Fig. 5A, B). A clear advantage of using  
 306 such a novel UV-VIS imaging technique over the other well-established imaging techniques  
 307 lies in the simplicity of operation and interpretation of generated data, analogous to findings  
 308 by Østergaard.[31] The measurement of light intensity passing through an area of a quartz tube  
 309 as a function of position and time can also enable quantification of the drug substance at  
 310 different time intervals. During the dissolution process, drug concentration increased in the  
 311 first 20 min in the closed loop of the flow-through system. Simultaneously the tablet size was  
 312 eroded at a rate of 16.4 and 15.2  $\mu\text{m}/\text{min}$  for horizontal and vertical planes respectively. It is  
 313 worth noting that surface analysis indicated no significant swelling in the first 5 min. The  
 314 simultaneous drug release data suggested that under the dissolution conditions of study, the  
 315 majority of drug release took place by a diffusion mechanism before the erosion of the  
 316 methacrylic matrix within the flow-through cell is complete.



318 **Figure 5.** Changes in tablet height (A) and width (B) at 0, 10, 20, 30, 40, 50 and 60 min of the flow  
 319 through dissolution test using Actipix SDI 2 dissolution imaging technology. (C) UV absorbance image  
 320 following the illumination of follow cell containing warfarin 3D printed tablet at 255 nm wavelength.  
 321 (D) Percentage sodium warfarin release from 3D printed tablet during dissolution test (n=3,  $\pm$ SD).

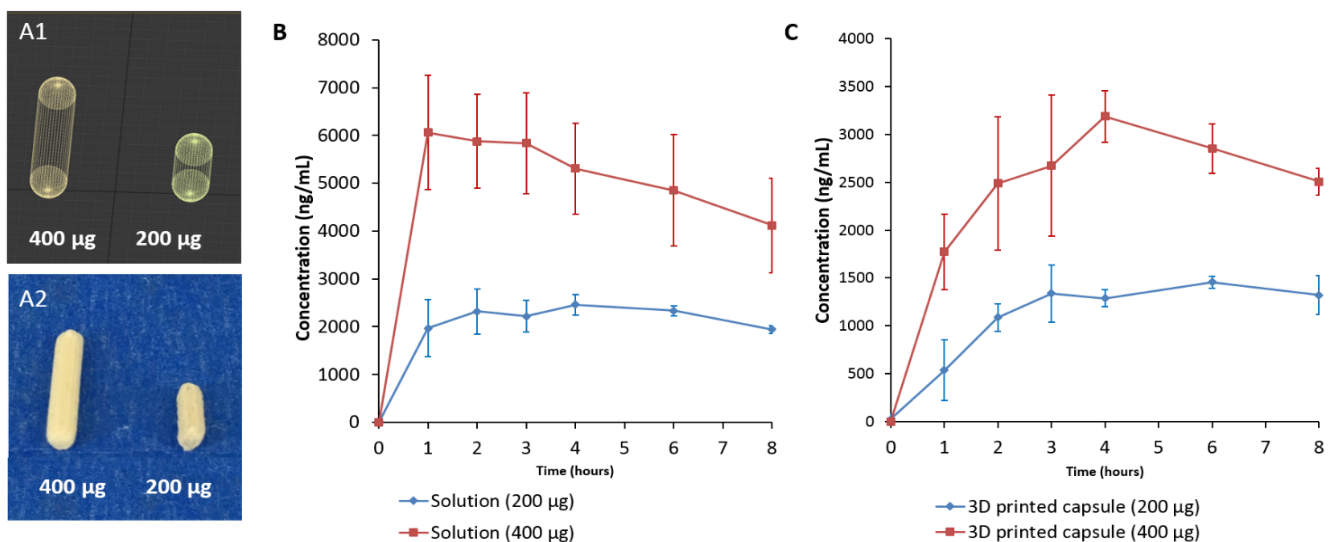
322 A prime advantage of 3D printing technologies lies in their highly flexible nature and  
 323 capacity to construct dosage forms with accurate spatial distribution of ingredients compared  
 324 to traditional manufacturing techniques. Therefore, constructs can now be printed to suit the  
 325 anatomy of not only a particular animal but according to the weight and size of that subject.  
 326 Rats are commonly considered most suitable for determining the mechanism of drug absorption  
 327 and bioavailability values from powder or solution formulations [32] as well as micro- or nano-  
 328 particles [33].

329 Two different warfarin tablets were specially designed (Fig. 6A1) to mimic the dimensions  
 330 of commonly used hard capsules intended for oral delivery to rats. Tablets were successfully  
 331 printed (Fig. 6A2) and were orally gavaged to rats. The pharmacokinetic parameters of warfarin  
 332 following oral administration either as 3D printed tablets or in a solution form were evaluated  
 333 (Table 1, Fig. 6B, C). Warfarin plasma exposure was significantly different when an equal dose  
 334 was administered either as solutions or as 3D printed tablets. The solution showed a markedly  
 335 higher  $C_{max}$  (2.5 and 6.44 mg/mL) and shorter  $T_{max}$  (2.67 or 1.5h) for the 200 or 400  $\mu$ g/mL  
 336 solution respectively, in comparison to  $C_{max}$  values (1.51 and 3.33 mg/mL) and  $T_{max}$  values (6  
 337 or 3.7 h) for 200  $\mu$ g ( $p < 0.05$ ) and 400  $\mu$ g ( $p < 0.01$ ) warfarin tablets respectively.

339 **Table 1.** Summary of pharmacokinetic parameters of warfarin following oral gavage of 200 or 400µg  
 340 from sodium warfarin solution and 3D printed tablets to adult healthy male Sprague–Dawley rats.

Dose	C <sub>max</sub> * (µg/mL)	T <sub>max</sub> * (h)	AUC <sub>1-8</sub> * (mg/mL.h)
Solution (200 µg)	2.5±0.3	2.67±1.15	20.64±1.9
Solution (400 µg)	6.44±0.1	1.5±0.6	39.56±7.4
3D printed tablet (200 µg)	1.51±0.09	6±1.6	10.8±2
3D printed tablet (400 µg)	3.33±0.5	3.7±1	19.93±1

341 \* C<sub>max</sub>, Maximum serum concentration; T<sub>max</sub>, Time at which C<sub>max</sub> is observed; and AUC<sub>1-8</sub>, area under  
 342 curve.  
 343



344 **Figure 6. (A1)** Rendered images and **(A2)** photographs of purpose designed 3D printed tablets for oral  
 345 gavage in rats, **(B)** Plasma concentration- time profile of warfarin following the oral dosing of 200 or  
 346 400µg from **(B)** warfarin solution and **(C)** warfarin loaded 3D printed tablets to adult healthy male  
 347 Sprague–Dawley rats (n=4), error bars ±SD.

348 Contributing to the finding above, the additional erosion step of Eudragit E in the 3D printed  
 349 tablets is thought to slow down the release of warfarin from the tablets.. In reality, in an *in vivo*  
 350 situation, dissolution is expected to be slower than suggested by *in vitro* dissolution techniques  
 351 since a significantly higher pH of the stomach contents in rats pH 3.2 (fed) and pH 3.9 (fasted)  
 352 [34] exists compared to the *in vitro* human simulation media conditions. Furthermore, the low  
 353 fluid volume (3.2±1.8 mL) in the fasted rats are likely to contribute to slower dissolution rates  
 354 of the methacrylate polymer *in vivo* than *in vitro*. The longer T<sub>max</sub> of the tablets might also be  
 355 attributed to the slower transit time of the relatively large oral units in rodents as previously  
 356 observed to be the case for oral pellets. Such effects are likely to be minimal in healthy human  
 357 adults where greater volumes of gastric fluids [35, 36] and a lower pH [37] at fasted state are  
 358 known. In summary, when extrapolating the findings to the human situation, it should be  
 359 considered that such delay has been augmented by the slower erosion of cationic polymer is  
 360 rat gastric environments rats due to their relatively higher gastric pH and lower fluid contents  
 361 in comparison to humans. A key driver in the uptake and use of these polymer-rich tablets

362 (yielded by FDM 3D printing) is that they match the release from standard compressed  
363 powdered tablets. The data we present suggests that dissolution of 3D tablets requires  
364 acceleration. However recently, there has been reports of utilizing 3D printer geometry to  
365 fabricate tablet with complex structure to accelerate drug release [38, 39].  
366

367 On the other hand, 3D printed tablets were proportionately effective as solution  
368 formulations, in that a doubling of warfarin dose from the either tablet or solution resulted in a  
369 rough doubling of measured plasma exposure with AUC<sub>1-8</sub> values doubling from 20.64±1.9 to  
370 39.56±7.4 µg/mL for the 200 and 400 µg/mL solutions respectively and from 10.8±2 to  
371 19.93±1 µg/mL for the 200 and 400 µg 3D printed capsules, respectively (184 % versus 192%  
372 respectively). Envisioning a future scenario, a healthcare staff member may be able to use  
373 computer software to digitally directly tailor and manufacture an individualised precision dose  
374 and consequently provide plasma levels of warfarin appropriate to an individual patient's need.

375 In summary, the findings in this study clearly demonstrate the potential of 3D printing as a  
376 platform to design animal-suitable solid dosage forms and thus in principle provide a pathway  
377 for human use with the potential advantage of digitally titrating an individuals dose in response  
378 to clinical data. We have also shown the utility of a novel dissolution imaging system to give  
379 mechanistic insights into the dissolution process of a 3D-printed tablet dosage form.

380

381 **4. Conclusions**

382 This study demonstrates the flexibility of FDM 3D printers to fabricate solid dosage forms  
383 to purposely suit the anatomy of an animal subject. UV imaging indicated that the erosion of  
384 methacrylic matrix takes place at 16.4 and 15.2  $\mu\text{m}/\text{min}$  for horizontal and vertical planes  
385 respectively and resulted in delayed plasma exposure in comparison to warfarin solutions.  
386 Moreover, the titration of dose of a narrow therapeutic index drug, warfarin, has been  
387 demonstrated *in vitro* and *in vivo*. In principle, the technology holds the promise to provide a  
388 much more dynamic and responsive anticoagulant regime to suit a constantly changing  
389 patient's INR profile. Such an approach can provide patients with a safer, more accurate and  
390 computerised alternative to the more commonly used approach of dosing using multiple tablets  
391 to include tablet splitting.

392 **Acknowledgments**

393 The authors would like to thank UCLAN Innovation Team for this support and Mrs Reem  
394 Arafat for her help with graphics design.

395 **Conflicts of interest** M A Alhnan is the innovator in patent applications WO 2016038356  
396 A1, WO2017072536A1 and WO2018020237A1 in the field of 3D printing of medicines.

397 **References**

- 398 [1] K.A. Bauer, Pros and cons of new oral anticoagulants, ASH Education Program Book, 2013  
399 (2013) 464-470.
- 400 [2] H. Takahashi, H. Echizen, Pharmacogenetics of CYP2C9 and interindividual variability in  
401 anticoagulant response to warfarin, *Pharmacogenomics J*, 3 (2003) 202-214.
- 402 [3] L.A. Linkins, P.T. Choi, J.D. Douketis, Clinical impact of bleeding in patients taking oral  
403 anticoagulant therapy for venous thromboembolism: a meta-analysis, *Ann Intern Med*, 139  
404 (2003) 893-900.
- 405 [4] J. Hirsh, J. Dalen, D.R. Anderson, L. Poller, H. Bussey, J. Ansell, D. Deykin, Oral  
406 anticoagulants: mechanism of action, clinical effectiveness, and optimal therapeutic range,  
407 *Chest*, 119 (2001) 8S-21S.
- 408 [5] M. Kuruvilla, C. Gurk-Turner, A review of warfarin dosing and monitoring, *Proceedings*  
409 (Baylor University. Medical Center), 14 (2001) 305-306.
- 410 [6] S.W. Hill, A.S. Varker, K. Karlage, P.B. Myrdal, Analysis of drug content and weight  
411 uniformity for half-tablets of 6 commonly split medications, *J Manag Care Pharm*, 15 (2009)  
412 253-261.
- 413 [7] J.E. Polli, S. Kim, B.R. Martin, Weight uniformity of split tablets required by a Veterans  
414 Affairs policy, *J Manag Care Pharm*, 9 (2003) 401-407.
- 415 [8] P.R. Vuddanda, M. Alomari, C.C. Doodoo, S.J. Trenfield, S. Velaga, A.W. Basit, S. Gaisford,  
416 Personalisation of warfarin therapy using thermal ink-jet printing, *Eur J Pharm Sci*, 117 (2018)  
417 80-87.
- 418 [9] T.C. Okwuosa, D. Stefaniak, B. Arafat, A. Isreb, K.W. Wan, M.A. Alhnan, A Lower  
419 Temperature FDM 3D Printing for the Manufacture of Patient-Specific Immediate Release  
420 Tablets, *Pharm Res*, 33 (2016) 2704-2712.
- 421 [10] J. Skowrya, K. Pietrzak, M.A. Alhnan, Fabrication of extended-release patient-tailored  
422 prednisolone tablets via fused deposition modelling (FDM) 3D printing, *Eur J Pharm Sci*, 68  
423 (2015) 11-17.
- 424 [11] A. Goyanes, P. Robles Martinez, A. Buanz, A.W. Basit, S. Gaisford, Effect of geometry on  
425 drug release from 3D printed tablets, *Int J Pharm*, 494 (2015) 657-663.
- 426 [12] K. Pietrzak, A. Isreb, M.A. Alhnan, A flexible-dose dispenser for immediate and extended  
427 release 3D printed tablets, *Eur J Pharm Biopharm*, 96 (2015) 380-387.
- 428 [13] A. Goyanes, H. Chang, D. Sedough, G.B. Hatton, J. Wang, A. Buanz, S. Gaisford, A.W. Basit,  
429 Fabrication of controlled-release budesonide tablets via desktop (FDM) 3D printing, *Int J*  
430 *Pharm*, 496 (2015) 414-420.
- 431 [14] T.C. Okwuosa, B.C. Pereira, B. Arafat, M. Cieszynska, A. Isreb, M.A. Alhnan, Fabricating a  
432 Shell-Core Delayed Release Tablet Using Dual FDM 3D Printing for Patient-Centred Therapy,  
433 *Pharm Res*, 34 (2017) 427-437.
- 434 [15] M. Sadia, A. Sosnicka, B. Arafat, A. Isreb, W. Ahmed, A. Kelarakis, M.A. Alhnan, Adaptation  
435 of pharmaceutical excipients to FDM 3D printing for the fabrication of patient-tailored  
436 immediate release tablets, *Int J Pharm*, 513 (2016) 659-668.
- 437 [16] X. Cao, S.T. Gibbs, L. Fang, H.A. Miller, C.P. Landowski, H.C. Shin, H. Lennernas, Y. Zhong,  
438 G.L. Amidon, L.X. Yu, D. Sun, Why is it challenging to predict intestinal drug absorption and  
439 oral bioavailability in human using rat model, *Pharm Res*, 23 (2006) 1675-1686.
- 440 [17] D. Mann, US Patent 4637816 A: Apparatus for the oral administration of capsules to  
441 animals, in, 1987.

442 [18] Z. Atcha, C. Rourke, A.H. Neo, C.W. Goh, J.S. Lim, C.C. Aw, E.R. Browne, D.J. Pemberton,  
443 Alternative method of oral dosing for rats, *J Am Assoc Lab Anim Sci*, 49 (2010) 335-343.

444 [19] A. Vetter, G. Perera, K. Leithner, G. Klima, A. Bernkop-Schnurch, Development and in vivo  
445 bioavailability study of an oral fondaparinux delivery system, *Eur J Pharm Sci*, 41 (2010) 489-  
446 497.

447 [20] J.Y. Kim, H.J. Bae, J. Choi, J.R. Lim, S.W. Kim, S.H. Lee, E.S. Park, Efficacy of gastro-retentive  
448 forms of ecabet sodium in the treatment of gastric ulcer in rats, *Arch Pharm Res*, 37 (2014)  
449 1053-1062.

450 [21] N. Sandler, I. Kassamakov, H. Ehlers, N. Genina, T. Ylitalo, E. Haeggstrom, Rapid  
451 interferometric imaging of printed drug laden multilayer structures, *Sci Rep*, 4 (2014) 4020.

452 [22] Brian R. Genge, Licia Wu, Glenn R. Sauer, Roy E. Wuthier, R. Genge, US Patent 7527687  
453 B2 Biocompatible cement containing reactive calcium phosphate nanoparticles and methods  
454 for making and using such cement., in, 2009.

455 [23] A. Nguyenpho, A.B. Ciavarella, A. Siddiqui, Z. Rahman, S. Akhtar, R. Hunt, M. Korang-  
456 Yeboah, M.A. Khan, Evaluation of In-Use Stability of Anticoagulant Drug Products: Warfarin  
457 Sodium, *J Pharm Sci*, 104 (2015) 4232-4240.

458 [24] Z. Rahman, M. Korang-Yeboah, A. Siddiqui, A. Mohammad, M.A. Khan, Understanding  
459 effect of formulation and manufacturing variables on the critical quality attributes of warfarin  
460 sodium product, *Int J Pharm*, 495 (2015) 19-30.

461 [25] S.A. Khaled, J.C. Burley, M.R. Alexander, C.J. Roberts, Desktop 3D printing of controlled  
462 release pharmaceutical bilayer tablets, *Int J Pharm*, 461 (2014) 105-111.

463 [26] D.-G. Yu, C. Branford-White, Y.-C. Yang, L.-M. Zhu, E.W. Welbeck, X.-L. Yang, A novel fast  
464 disintegrating tablet fabricated by three-dimensional printing, *Drug Dev Ind Pharm*, 35 (2009)  
465 1530-1536.

466 [27] W.E. Katstra, R.D. Palazzolo, C.W. Rowe, B. Giritlioglu, P. Teung, M.J. Cima, Oral dosage  
467 forms fabricated by Three Dimensional Printing™, *J Control Release*, 66 (2000) 1-9.

468 [28] A. Aburub, D.S. Risley, D. Mishra, A critical evaluation of fasted state simulating gastric  
469 fluid (FaSSGF) that contains sodium lauryl sulfate and proposal of a modified recipe, *Int J*  
470 *Pharm*, 347 (2008) 16-22.

471 [29] B. comission, British Pharmacopeia 2017, The British Pharmacopoeia Commission (BCP)  
472 Office, London, 2017.

473 [30] W.L. Hulse, J. Gray, R.T. Forbes, A discriminatory intrinsic dissolution study using UV area  
474 imaging analysis to gain additional insights into the dissolution behaviour of active  
475 pharmaceutical ingredients, *Int J Pharm*, 434 (2012) 133-139.

476 [31] J. Ostergaard, UV imaging in pharmaceutical analysis, *J Pharm Biomed Anal*, (2017).

477 [32] T.T. Kararli, Comparison of the Gastrointestinal Anatomy, Physiology, and Biochemistry  
478 of Humans and Commonly Used Laboratory-Animals, *Biopharmaceutics & Drug Disposition*,  
479 16 (1995) 351-380.

480 [33] M. Mori, Y. Shirai, Y. Uezono, T. Takahashi, Y. Nakamura, H. Makita, Y. Nakanishi, Y.  
481 Imasato, Influence of specific gravity and food on movement of granules in the  
482 gastrointestinal tract of rats, *Chem Pharm Bull (Tokyo)*, 37 (1989) 738-741.

483 [34] E.L. McConnell, A.W. Basit, S. Murdan, Measurements of rat and mouse gastrointestinal  
484 pH, fluid and lymphoid tissue, and implications for in-vivo experiments, *J Pharm Pharmacol*,  
485 60 (2008) 63-70.

486 [35] F. Gotch, J. Nadell, I.S. Edelman, Gastrointestinal water and electrolytes. IV. The  
487 equilibration of deuterium oxide (D<sub>2</sub>O) in gastrointestinal contents and the proportion of  
488 total body water (T.B.W.) in the gastrointestinal tract, *J Clin Invest*, 36 (1957) 289-296.  
489 [36] C. Tuleu, C. Andrieux, P. Boy, J.C. Chaumeil, Gastrointestinal transit of pellets in rats:  
490 effect of size and density, *Int J Pharm*, 180 (1999) 123-131.  
491 [37] D.F. Evans, G. Pye, R. Bramley, A.G. Clark, T.J. Dyson, J.D. Hardcastle, Measurement of  
492 gastrointestinal pH profiles in normal ambulant human subjects, *Gut*, 29 (1988) 1035-1041.  
493 [38] M. Kyobula, A. Adedeji, M.R. Alexander, E. Saleh, R. Wildman, I. Ashcroft, P.R. Gellert, C.J.  
494 Roberts, 3D inkjet printing of tablets exploiting bespoke complex geometries for controlled  
495 and tuneable drug release, *J Control Release*, 261 (2017) 207-215.  
496 [39] M. Sadia, B. Arafat, W. Ahmed, R.T. Forbes, M.A. Alhnan, Channelled tablets: An  
497 innovative approach to accelerating drug release from 3D printed tablets, *J Control Release*,  
498 269 (2018) 355-363.

#### 499 **List of Figures**

500

501 **Figure 1.** Schematic diagram of SDi2 instrument. LED's of different wavelength are employed to  
502 illuminate the 3D printed tablet in flow through cell filled with gastric medium. The obscuration or  
503 absorbance of the sample was recorded using an Actipix detector. The medium is pre-heated to 37°C  
504 before going through the Whole Dosage Flow Cell and is recirculated in a closed loop configuration.

505 **Figure 2.** Precision of 3D printing to control low dose sodium warfarin. **(A)** Images of warfarin loaded  
506 FDM 3D printed tablets with increasing dose, **(B)** Correlation between the theoretical volume and  
507 tablet mass, **(C)** warfarin dose accuracy in the 3D printed tablets and **(D)** correlation between  
508 theoretical volume and warfarin dose (n=3, ±SD).

509 **Figure 3.** Thermal analysis of Eudragit E based 3D printing filaments. **(A)** Thermal degradation profiles  
510 for Eudragit E, sodium warfarin, TCP, warfarin loaded filament and tablet, **(B)** DSC thermograph for  
511 warfarin loaded filament and tablet, **(C)** XRD spectra of Eudragit E, TCP, warfarin, and warfarin loaded  
512 filament and tablet.

513 **Figure 4.** *In vitro* release pattern of sodium warfarin from 3D printed tablets of different doses from a  
514 USP II dissolution test in modified FaSSGF (pH 2.0) (n=3, ±SD).

515 **Figure 5.** Changes in tablet height **(A)** and width **(B)** at 0, 10, 20, 30, 40, 50 and 60 min of the flow  
516 through dissolution test using Actipix SDI 2 dissolution imaging technology. **(C)** UV absorbance image  
517 following the illumination of flow cell containing warfarin 3D printed tablet at 255 nm wavelength.  
518 **(D)** Percentage sodium warfarin release from 3D printed tablet during dissolution test (n=3, ±SD).

519 **Figure 6. (A1)** Rendered images and **(A2)** photographs of purpose designed 3D printed tablets for  
520 oral gavage in rats, **(B)** Plasma concentration- time profile of warfarin following the oral dosing of  
521 200 or 400µg from **(B)** warfarin solution and **(C)** warfarin loaded 3D printed tablets to adult healthy  
522 male Sprague–Dawley rats (n=4), error bars ±SD.

#### 523 **List of tables**

524 **Table 1.** Summary of pharmacokinetic parameters of warfarin following oral gavage of 200 or 400µg  
525 from sodium warfarin solution and 3D printed tablets to adult healthy male Sprague–Dawley rats.

#### 526 **Supplementary data**

527 **Table 1S.** Summary of length, width, height and volume of cuboid containing warfarin loaded 3D  
528 printed tablets.

529

530 **Tailored on demand anti-coagulant dosing: an *in vitro* and *in***  
531 ***vivo* evaluation of 3D printed purpose-designed oral dosage**  
532 **forms**

533

534 Basel Arafat<sup>1,2</sup>, Nidal Qinna<sup>2</sup> Milena Cieszynska<sup>1</sup>, Robert T Forbes<sup>1</sup>, Mohamed A  
535 Alhnan<sup>1\*</sup>

536

537 <sup>1</sup>School of Pharmacy and Biomedical Sciences and <sup>2</sup>School of Medicine, University of Central  
538 Lancashire, Preston, Lancashire, UK.

539 <sup>2</sup> Faculty of Pharmacy and Medical Sciences, University of Petra, Amman, Jordan.

540

## 541 **Supplementary Data**

542

543

544

545

546 \*Corresponding author: [MAIbedAlhnan@uclan.ac.uk](mailto:MAIbedAlhnan@uclan.ac.uk)

547

548

549

550

551 **Table 1S.** Summary of length, width, height and volume of cuboid containing sodium warfarin loaded  
552 3D printed tablets

553

<b>Target dose (µg)</b>	<b>Volume (mm<sup>3</sup>)</b>	<b>X (mm)</b>	<b>Y (mm)</b>	<b>Z (mm)</b>
<b>300</b>	19.06	5.09	1.86	2.00
<b>500</b>	40.74	6.55	2.40	2.58
<b>1000</b>	94.93	8.68	3.18	3.42
<b>1500</b>	149.12	10.09	3.69	3.98
<b>2000</b>	203.31	11.19	4.09	4.41
<b>2500</b>	257.51	12.10	4.43	4.77
<b>3000</b>	311.70	12.90	4.72	5.08
<b>4000</b>	420.08	14.24	5.21	5.61
<b>5000</b>	528.47	15.38	5.62	6.06

554

555

556